

# Evaluation of the Effect of Needle Tilting Angle on Irrigant Flow in the Root Canal Using Side-Vented Needle by an Unsteady Computational Fluid Dynamics Model

Ozkan Adiguzel<sup>1</sup>, Mehmet Gokhan Gokcen<sup>2</sup>, Ali Bahadir Olcay<sup>3</sup>

<sup>1</sup> Dicle University, Faculty of Dentistry, Department of Endodontics, Diyarbakır, Turkey

<sup>2</sup> Dogus University, Faculty of Engineering, Department of Mechanical Engineering, İstanbul, Turkey

<sup>3</sup> Yeditepe University, Faculty of Engineering, Department of Mechanical Engineering, İstanbul, Turkey

## Correspondence:

Ozkan ADIGUZEL  
Dicle University,  
Faculty of Dentistry,  
Department of Endodontics,  
21280, Diyarbakır, TURKEY.  
e-mail: ozkanadiguzel@dicle.edu.tr

Received 7 December 2015

Accepted 10 March 2016

Access Online



DOI  
10.5577/intdentres.  
2016.vol6.no1.1

## Abstract

**Aim:** The Irrigant flow dynamics has strong influence on the root canal cleaning effectiveness. The aim of this study was to evaluate the effect of needle tilting angle on irrigant flow inside a prepared root canal during final irrigation with a side-vented needle using a validated Computational Fluid Dynamics (CFD) model.

**Methodology:** To analyze the irrigant flow a CFD model with tilting angles of 0 and 2 degrees was created. The irrigant flow in the apical root canal was simulated. Computations were carried out for two selected flow rates of 0.26 and 0.78 mL/s to evaluate the velocity and turbulence quantities along the solution domain.

**Results:** In addition to velocity and pressure distribution at the apex, wall shear stress distribution, vorticity and turbulent intensity results were obtained for needle tilting angle of 0 and 2 degrees. In the case of turbulent flows where the flow rate was higher, irrigation is better; however, higher apical pressures were observed for both tilting angles. Although the effect of tilting angle of two degrees for laminar flow was slightly better than zero degrees, the effect of tilting was significant for the turbulent flow case. Wall shear stress distribution, vorticity and turbulent intensity results were consistent with each other.

**Conclusions:** A small tilting angle of 2 degrees had an effect on irrigation effectiveness which could be clearly observed from the wall shear stress, vorticity and velocity distribution results. The velocity distribution results obtained at the symmetry plane should be evaluated with the wall shear stress values together to observe the complete fluid dynamics structure inside the root canal.

**Keywords:** Computational Fluid Dynamics, side-vented needle, irrigation, tilting angle, laminar, turbulent model

**How to cite this article:** Adiguzel O, Gokcen MG, Olcay AB. Evaluation of the Effect of Needle Tilting Angle on Irrigant Flow in the Root Canal Using Side-Vented Needle by an Unsteady Computational Fluid Dynamics Model. Int Dent Res 2016;6:1-8.

## Introduction

The success of root canal treatment depends on thorough chemo-mechanical procedures which are mainly accomplished by irrigation and biomechanical preparation of the root canal system (1-3). Approximately, 40–50% of the root canal wall surface remains uninstrumented during preparation due to the root canals' complex anatomy and this eventually yields insufficient debridement (4).

Conventional irrigant injection with syringes has been recommended as an efficient irrigation method (5). Needles are designed to deliver the irrigant through their most distal end or laterally through side-vented channels (6). Side-vented endodontic irrigating needles which have a round tip and a side port allow some of the pressure to be transmitted straight out and some to be vented laterally (6).

Previous studies about the irrigation efficiency have mainly examined the removal efficiency of bacteria and debris. Besides, these studies focused on the flow pattern developed in the root canal that leads to preparation size and positioning of the needle closer to working length (7, 8). To date, there has been no reported investigation of the effect of needle tilting angle on irrigation protocol.

Computational Fluid Dynamics (CFD) is a powerful technique to simulate the fluid flow based on finite volume approximations of Navier-Stokes (i.e., governing fluid flow) equations (9-11). Due to its convenience, CFD model was recently introduced for the evaluation of irrigant flow in the root canal (12). CFD method enables a complex numeric analysis of root canal irrigation allowing the simulation of real physical conditions, and the determination of associated complex parameters (6, 12, 13). CFD simulations can also provide detailed velocity field, shear stress, and pressure solutions in case where experimental study is difficult (14).

The aim of this study was to evaluate the effect of needle tilting angle on irrigant flow inside a prepared root canal during final irrigation with a side-vented needle using a validated CFD model. Also, this study investigated mixing mechanism in the apical region and examined parameters that may have influence on efficient root canal cleaning.

## Materials and Methods

The geometry of the root canal is modeled with a conical frustum with the larger area at the canal outlet having a diameter of 1.59 mm and the smaller area at the apex having a diameter of 0.45 mm as shown in figure 1. The length of the root canal is 19 mm whereas the length of the apex is 0.5 mm. The apex is also modeled with an inverted conical frustum where the smaller area attached to the root

canal tip and having the diameter of 0.3 mm and the larger area has a diameter of 0.35 mm.

The needle is modeled based on the geometry of commercially available 30-G side-vented endodontic irrigation needle (KerrHawe Irrigation Probe, KerrHawe SA, Bioggio, Switzerland). The external diameter of the needle is measured to be 320  $\mu\text{m}$  and the internal diameter is taken as 196  $\mu\text{m}$ . The length of the needle is measured as 31 mm. While the needle tip is placed at a distance of 3 mm from the apex center, 15 mm part of the needle is left outside the root canal. The tilting angle  $\alpha$  is defined as the angle between the axis of the conical frustum and the needle axis as shown in figure 1. The angle  $\alpha$  is set to 0.0° or 2.0° while 2.0° is being the geometrical limit.

Reynolds number is a non-dimensional number used for identifying flow characteristics in any given flow. While Reynolds number briefly states the ratio of inertial forces to viscous forces, low Reynolds number flows are considered to be laminar due to the effect of viscous forces. Similarly, high Reynolds number flows are governed by inertial forces and being considered as turbulent (15).

In this study, needle Reynolds number is defined as

$$Re = \frac{\rho V D}{\mu}$$

where  $\rho$  is the fluid density,  $\mu$  is fluid's dynamic viscosity,  $V$  is the fluid mean velocity and  $D$  is the diameter of the needle. The irrigation fluid is considered as distilled water with density of 998.2 kg/m<sup>3</sup>, dynamic viscosity of 0.001003 kg/m\*s and needle diameter is taken to be 0.196 mm. To simulate a typical syringe injection, 2 mL of fluid is provided inside the needle and simulations are performed for clinically realistic volumetric flow rates of 0.26 mL/s and 0.78 mL/s. The volumetric flow rate of 0.26 mL/s corresponds to laminar flow with Reynolds number of 1678 and the flow velocity is 8.62 m/s whereas the volumetric flow rate of 0.78 mL/s corresponds to turbulent flow with Reynolds number of 5034 and the flow velocity is 25.86 m/s. Turbulent flow analysis has been performed using shear stress transport (SST)  $k-\omega$  model as mentioned by Gao et. al (13).

To simulate the irrigation fluid in the root canal, needle entrance is defined as velocity inlet with flat velocity profile while ambient pressure condition is imposed on the root canal orifice as shown in figure 1. The no-slip condition is enforced on the needle and root canal walls to take into account of viscosity. Gravity was taken in the direction of flow (i.e., +z axis). The flow evolution was simulated using three dimensional, unsteady, incompressible, Navier-Stokes equations, namely,

$$\frac{1}{r} \frac{\partial}{\partial r} (ru_r) + \frac{1}{r} \frac{\partial u_\theta}{\partial \theta} + \frac{\partial u_z}{\partial z} = 0$$

$$\frac{\partial u_r}{\partial t} + (\vec{u} \cdot \vec{\nabla})u_r - \frac{u_\theta^2}{r} = -\frac{1}{\rho} \frac{\partial p}{\partial r} + \nu \left( \nabla^2 u_r - \frac{u_r}{r^2} - \frac{2}{r^2} \frac{\partial u_\theta}{\partial \theta} \right)$$

$$\frac{\partial u_\theta}{\partial t} + (\vec{u} \cdot \vec{\nabla})u_\theta + \frac{u_r u_\theta}{r} = -\frac{1}{\rho r} \frac{\partial p}{\partial \theta} + \nu \left( \nabla^2 u_\theta - \frac{u_\theta}{r^2} + \frac{2}{r^2} \frac{\partial u_r}{\partial \theta} \right)$$

$$\frac{\partial u_z}{\partial t} + (\vec{u} \cdot \vec{\nabla})u_z = -\frac{1}{\rho} \frac{\partial p}{\partial z} + \nu \nabla^2 u_z$$

solver scheme was second order accurate and SIMPLE algorithm was used for pressure–velocity coupling. Simulations were run using commercial CFD code Ansys Fluent © version 13 (ANSYS, Inc., Pennsylvania, USA). A Dell Precision T5500 workstation (Dell Computers, Austin, TX, USA) consisting of Dual Intel Xeon E5630 processor each having quad core, 24GB DDR3 RAM and nVidia 1GB Quadro 2000 video card was dedicated to perform the simulations.

The governing equations were solved using a finite volume method with a fixed time step. The

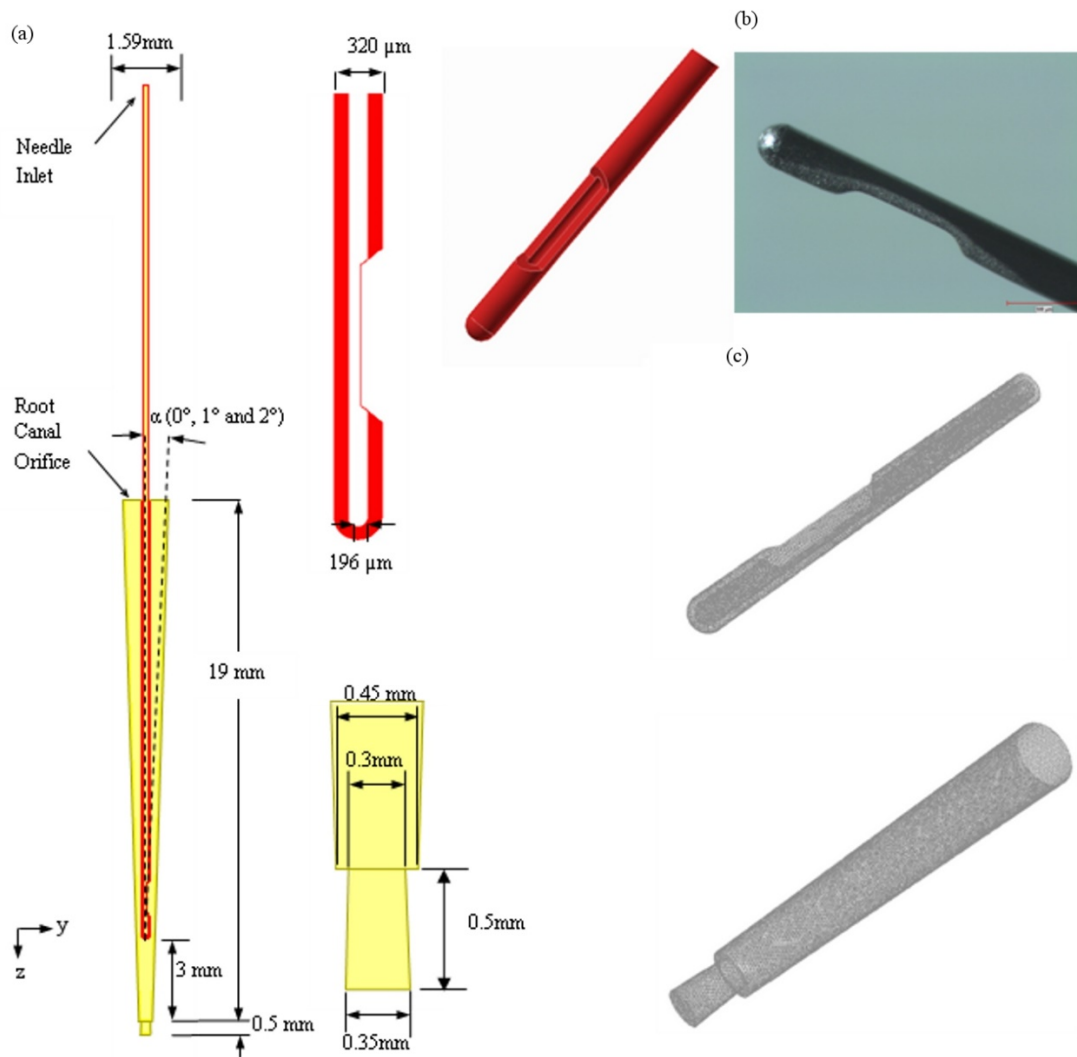


**Figure 1.** Solid model of the canal and the needle with dimensions (b) Image of the 30-G needle using Nikon SMZ 745 (Nikon, Melville, NY, USA) with 50x magnification, (c) Computational mesh.

Mesh convergence test has been performed in order to determine sufficient number of elements that would provide reasonable accuracy in the results. The more elements were placed near the needle and root canal walls since high velocity gradient is expected at these locations (i.e., near the

wall inside the boundary layer of flow field). The model consisted of 3.492 million tetrahedral elements with mean element volume of  $4.825 \times 10^{-6} \text{ mm}^3$ .

## Results

Figure 2A shows the velocity magnitude plots in y-z plane (i.e., symmetry plane) for laminar and turbulent flows when tilting angle,  $\alpha$ , is varied from  $0.0^\circ$  to  $2.0^\circ$ . It is observed that with increasing tilting angle, dead water zone seems to be decreasing for laminar flow while shows no difference for turbulent cases. Figure 2B, on the other hand, illustrates the velocity magnitude plots within enlarged view (i.e., the values below 0.01 m/s). Turbulent flow results on figure 2B (g) and (h)

clearly illustrate that regardless of tilting angle's value almost everywhere in the apex region has nonzero velocity if volumetric flow rate of 0.78 mL/s is used. Turbulent flows are inherently associated with chaotic and fluctuating behaviors eventually resulting in enhanced mixing in the flow fields. On the other hand, turbulent flows naturally would require more pressure than laminar flows for the same geometries. In other words, when turbulent flow is present in the apex region, we would expect to observe much more pressure than laminar case.

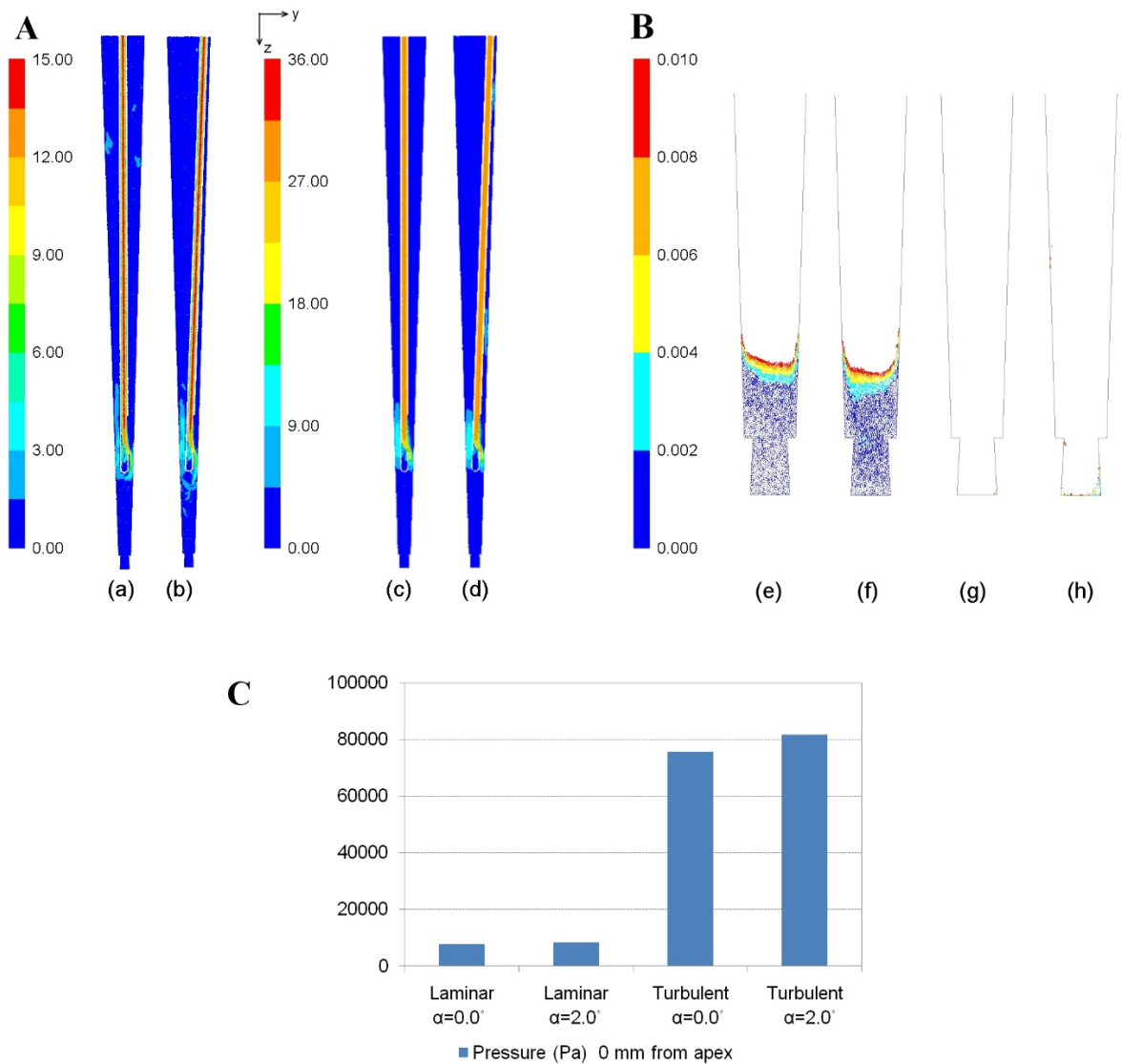


**Figure 2. A:** Velocity magnitude (m/s) plots: (a) laminar  $\alpha = 0.0^\circ$ , (b) laminar  $\alpha = 2.0^\circ$ , (c) turbulent  $\alpha = 0.0^\circ$ , (d) turbulent  $\alpha = 2.0^\circ$ . **B:** Enlarged view of figure 2A around apex region. Velocity magnitude (m/s) plots illustrating dead water zone region: (e) laminar  $\alpha = 0.0^\circ$ , (f) laminar  $\alpha = 2.0^\circ$ , (g) turbulent  $\alpha = 0.0^\circ$ , (h) turbulent  $\alpha = 2.0^\circ$ . **C:** Total pressure values at apical region when tilting angle is varied for laminar and turbulent flows.

Figure 2C shows the total pressure values at the apex. It can be seen that use of 0.78 mL/s instead of 0.26 mL/s causes almost 10 times more pressure at the apex region. Also, when tilting angle has been set to 2.0° for turbulent flow, pressure seems to be becoming 10% more than tilting angle of 0.0°. Laminar case pressure findings are in close agreement with Boutsoukis et. al (14, 16).

The wall shear stress,  $\tau_w$ , develops when there is a velocity gradient at any surface.  $\tau_w$  is related to the force parallel to the wall surface and given by

$$\tau_w = \mu \left( \frac{\partial V}{\partial n} \right)_{n=0},$$

where  $\mu$  is the dynamic viscosity,  $V$  is the flow velocity and  $n$  is normal coordinate from the wall.

The developed wall shear stress may be associated with the efficiency of the root canal wall cleaning because shear stress would indicate the intensity of sweeping of the wall surface.

Figure 3A shows the wall shear stress distribution at the root canal wall for less than 25 Pa. Thus, white color in the figure implies that surface is exposed to wall shear stress higher than 25 Pa. The comparison of figure 3A (a) and (b) suggest that the wall shear stress does not strongly depend on the tilting angle for the laminar flow while figure 3A (c) and (d) shows that the tilting angle has significant effect on the wall shear stress for the turbulent flow.

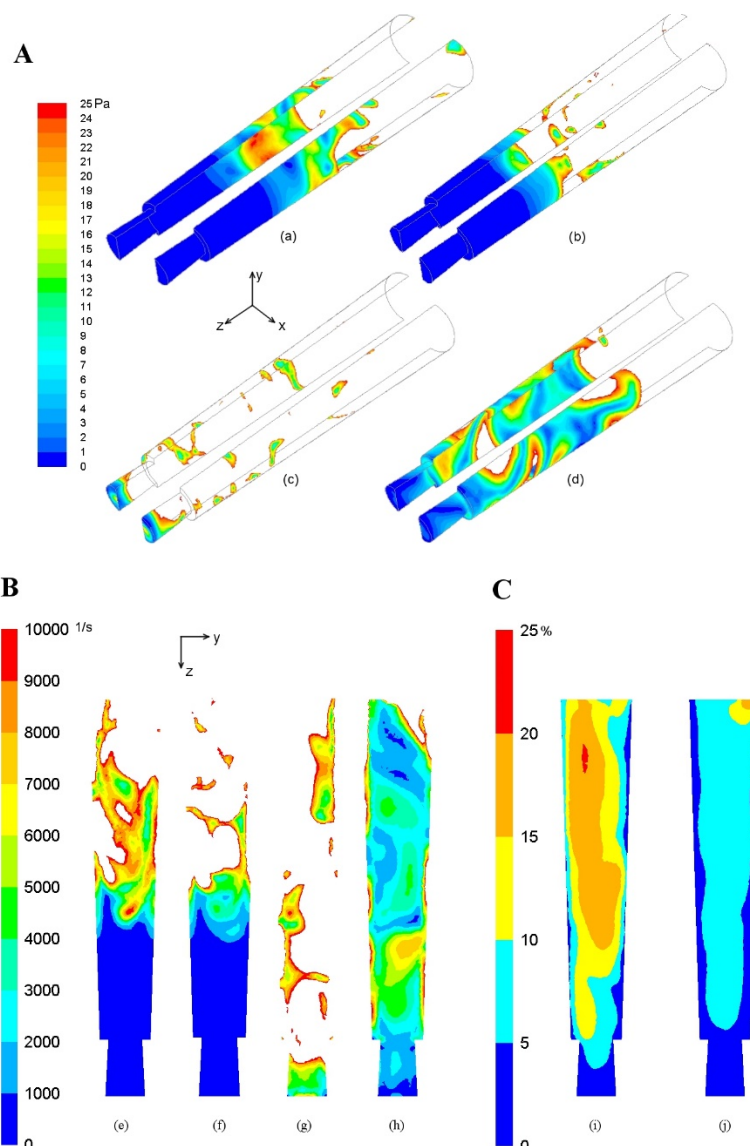


**Figure 3. A:** Wall shear stress (Pa) distribution at canal walls: (a) laminar  $\alpha = 0.0^\circ$ , (b) laminar  $\alpha = 2.0^\circ$ , (c) turbulent  $\alpha = 0.0^\circ$ , (d) turbulent  $\alpha = 2.0^\circ$ . **B:** Vorticity (1/s) plots at apical region (d) laminar  $\alpha = 0.0^\circ$ , (e) laminar  $\alpha = 2.0^\circ$ , (f) turbulent  $\alpha = 0.0^\circ$ , (g) turbulent  $\alpha = 2.0^\circ$ . **C:** Turbulent intensity (%) plots illustrating dead water zone region: (h) turbulent  $\alpha = 0.0^\circ$ , (i) turbulent  $\alpha = 2.0^\circ$ .

Vorticity is generally associated with the fluid particle's rotation in flow fields. Furthermore, in this study fluid particles rotation can enhance the circulation regions in the apical zone that can eventually increase the effectiveness of the root canal cleaning. Figure 3B shows the vorticity contour plots for laminar and turbulent flows when tilting angle is varied. It is observed that turbulent cases (figure 3B (g) and (h)) have clearly more vorticity compared to the laminar cases (figure 3B (e) and (f)). Also, when turbulent cases are examined, tilting angle of  $0.0^\circ$  (figure 3B (g)) has the stronger vorticity contours than the tilting angle of  $2.0^\circ$ . This may be related to the interaction of irrigation fluid with the root canal wall. When the fluid strikes to the root canal wall with steep angle, it would result in enhanced mixing that yields strong vorticities in the flow field. To investigate further on mixing authors looked into the turbulent intensity since this parameter is related to the turbulent velocity fluctuations which can improve the mixing in the flow field (Figure 3C). Turbulent intensity is defined as the ratio of the resultant velocity fluctuation to the resultant mean velocity. Therefore, high turbulent intensity implies that velocity fluctuations are large that yield enhanced mixing in the flow field. In this study, it is realized that tilting angle of  $0.0^\circ$  (figure 3C (i)) would provide more turbulent intensity compared to the other turbulent case with tilting angle of  $2.0^\circ$  (figure 3C (j)).

## Discussion

Studies on the effectiveness of the irrigation examined parameters including anatomy of the root canal geometry, size and curvature, volume, pressure and flow rate of irrigant, the type, design, size, diameter and insertion depth of the irrigation needle (8, 13, 17-22).

In the present study, a three-dimensional model of root canal irrigation, based on the geometry and physical characteristics of an in vitro model of side-vented needle irrigation, was numerically simulated, using validated commercial CFD code. No previous data has been reported concerning of the effect of needle tilting angle during root canal irrigation. This paper represents the effect of needle tilting angle on irrigation protocol.

In this study, turbulent flows clearly indicated that no dead water zone is present when 0.78 mL/s irrigation is performed. This finding is actually supported by Gulabivala et. al (15), as turbulence causes enhanced mixing that yields better irrigation efficiency. Therefore, in turbulent flows where the flow rate is higher, irrigation is better accompanied

with mixing, however, higher apical pressures are observed for both tilting angles. Specifically, when tilting angle is changed from zero to two degrees, apical pressure is raised about 10%. While turbulent pressure findings in the literature are not present at the time this study take place, laminar pressure findings are consistent with the data given in the literature (14, 16).

In addition to velocity magnitude and pressure plots at the apex region, wall shear stress distribution, vorticity and turbulent intensity results are also investigated to observe the effect of needle tilting angle. Authors believe that in order to understand the physics behind the root canal treatment, the study should examine the mixing mechanism inside root canal rather than solely velocity plots in the apical zone. Since vorticity is responsible for fluid rotation and inherently mixing, high vorticity cases (i.e., turbulent cases) provided more effective mixing in apical region compared to the laminar flow cases. When turbulent cases are evaluated for  $0.0^\circ$  and  $2.0^\circ$ ,  $0.0^\circ$  case results in more vorticity and turbulent intensity because flow exiting the needle strikes root canal wall with a steeper angle and bounces back instead of orienting towards the apex. This result is not apparent from velocity vector plots since rotation and mixing of fluid particles can not be clearly identified from velocity vector information.

On the other hand, wall shear stress is directly related to the irrigation fluid's washing or sweeping capability of a root canal wall. Besides, wall shear stress on the root canal surface may have an influence on the mechanical dissociation of debris, tissue remnants, biofilm, isolated microbes, and their byproducts. Since wall shear stress strongly depends on the velocity gradient, velocity distribution results should be evaluated together with the wall shear stress results. Particularly, velocity plots only give information about the bulk movement of the irrigation fluid whether it is moving towards the apex region or going up to the root canal orifice. In this study, although change in tilting angle seems to be making slight effect on irrigation from velocity plot, it is apparent that the tilting angle of zero degrees for turbulent case and two degrees for laminar case washes the root canal wall more efficiently than others based on wall shear stress results.

Even a small tilting angle which is difficult to differentiate by dental practitioner during the treatment may have strong influence on the irrigation because flow dynamics at the apical zone is mostly determined by the interaction between the flow leaving needle and the orientation of the root canal surface. Besides, increase in tilting angle may not necessarily mean that irrigation fluid would

reach further towards apex. Therefore, variation in tilting angle should be carefully examined.

Detailed information is needed about turbulence and flow distribution in the root canal system to understand the irrigation dynamics. While main parameters, such as flow velocity and apical pressure play a key role during root canal irrigation, vorticity, wall shear stress and turbulence intensity information illuminates the physics behind the irrigation flow in the root canal. This study particularly discusses the parameters affecting effectiveness of root canal treatment. As a result, findings in this paper can lead the determination of factors that can enhance or lessen the root canal treatment.

## Conclusions

Needle tilting angle was found to affect the extent of irrigant replacement and mixing, the shear stress on the root canal wall, dead water zone at the apical area, and the pressure at the apical foramen.

Computational Fluid Dynamics represents a powerful technique for the study of irrigant flow, in which experimental research is difficult to perform.

## Acknowledgments

*The authors deny any conflicts of interest related to this study.*

## References

1. Goldman LB, Goldman M, Kronman JH, Lin PS. The efficacy of several irrigating solutions for endodontics: a scanning electron microscopic study. *Oral Surg Oral Med Oral Pathol* 1981;52:197-204. [Crossref](#)
2. Abbott PV. The periapical space: a dynamic interface. *Aust Endodon J* 2002;28:96-107. [Crossref](#)
3. Ballal NV, Mala K and Bhat, KS. Effect of maleic acid and ethylenediaminetetraacetic acid on the dissolution of human pulp tissue – an in vitro study. *International Endodontic Journal*, 2011;44: 353–6. [Crossref](#)
4. Peters OA, Laib A, Göhring TN, Barbakow F. Changes in root canal geometry after preparation assessed by high-resolution computed tomography. *J Endod* 2001;27:1–6. [Crossref](#)
5. van der Sluis LW, Gambarini G, Wu MK, et al. The influence of volume, type of irrigant and flushing method on removing artificially placed dentine debris from the apical root canal during passive ultrasonic irrigation. *Int Endod J* 2006;39:472–6. [Crossref](#)
6. Shen Y, Gao Y, Qian W, et al. Three-dimensional numeric simulation of root canal irrigant flow with different irrigation needles. *J Endod*. 2010;36:884–9. [Crossref](#)
7. Albrecht LJ, Baumgartner JC, Marshall JG. Evaluation of apical debris removal using various sizes and tapers of ProFile GT files. *Journal of Endodontics* 2004;30:425–8. [Crossref](#)
8. Usman N, Baumgartner JC, Marshall JG. Influence of instrument size on root canal debridement. *Journal of Endodontics* 2004;30:110–2. [Crossref](#)
9. Tilton JN. Fluid and particle dynamics. In: Perry RH, Green DW, Maloney JO, eds. *Perry's Chemical Engineer's Handbook*. 7th ed. New York, NY: McGraw-Hill; 1999:1–50.
10. Arvand A, Hormes M, Reul H. A validated computational fluid dynamics model to estimate hemolysis in a rotary blood pump. *Artif Org* 2005;29:531–40. [Crossref](#)
11. Lecrivain G, Slaouti A, Payton C, et al. Using reverse engineering and computational fluid dynamics to investigate a lower arm amputee swimmer's performance. *J Biomech* 2008;41:2855–9. [Crossref](#)
12. Boutsioukis C, Lambrianidis T, Kastrinakis E. Irrigant flow within a prepared root canal using different flow rates: a computational fluid dynamics study. *Int Endod J* 2009;42:144–55. [Crossref](#)
13. Gao Y, Haapasalo M, Shen Y, et al. Development and validation of a three-dimensional computational fluid dynamics model of root canal irrigation. *J Endod* 2009;35:1282–7. [Crossref](#)
14. Boutsioukis C, Verhaagen B, Versluis M, et al. Evaluation of irrigant flow in the root canal using different needle types by an unsteady computational fluid dynamics model. *J Endod*. 2010;36:875–9. [Crossref](#)
15. Gulabivala K, Ng Y-L, Gilbertson M and Eames I. The fluid mechanics of root canal irrigation. *Physiol. Meas.* 2010;31:R49–R84. [Crossref](#)
16. Boutsioukis C, Lambrianidis T, Verhaagen B, et al. The Effect of Needle-insertion Depth on the Irrigant Flow in the Root Canal: Evaluation Using an Unsteady Computational Fluid Dynamics Model. *J Endod*. 2010;36:1664–8. [Crossref](#)
17. Boutsioukis C, Lambrianidis T, Kastrinakis E, et al. Measurement of pressure and flow rates during irrigation of a root canal ex vivo with three endodontic needles. *Int Endod J* 2007;40:504–13. [Crossref](#)
18. Khademi A, Yazdizadeh M, Feizianfard M. Determination of the minimum instrumentation size for penetration of irrigants to the apical third of root canal systems. *J Endod* 2006;32:417–20. [Crossref](#)

19. Vinothkumar TS, Kavitha S, Lakshminarayanan L, et al. Influence of irrigating needle-tip designs in removing bacteria inoculated into instrumented root canals measured using single-tube luminometer. *J Endod* 2007;33:746–8. [Crossref](#)
20. Yiğit Özer S, Adiguzel Ö, Kaya S. Removal of Debris and Smear Layer in Curved Root Canals Using Self-Adjusting File with Different Operation Times – A Scanning Electron Microscope Study. *Int Dent Res* 2011;1:1-6. [Crossref](#)
21. KW, Sedgley CM. The influence of preparation size on the mechanical efficacy of root canal irrigation in vitro. *J Endod* 2005;31:742–5. [Crossref](#)
22. Adiguzel Ö. A Literature Review of Self Adjusting File. *Int Dent Res* 2011;1:18-25. [Crossref](#)